MARS IN CONTEXT: COMPARATIVE ATMOSPHERIC CIRCULATION OF TERRESTRIAL PLANETS.

P. L. Read, *(peter.read@physics.ox.ac.uk)*, **F. Tabataba-Vakili, A. Valeanu, Y. Wang, R. M. B. Young,** *Department of Physics, University of Oxford, UK*.

Introduction

An understanding of the dominant factors and mechanisms controlling the general circulation of a planetary atmosphere is a prerequisite to our understanding of the climate variability of planets such as Mars and the Earth, both in the past and in the future. Without such an understanding, one cannot be sure that a particular model formulation is capable of representing or predicting how an atmosphere will respond to forcing conditions that may differ markedly from those of the present day. But the verification of a model used under such different conditions from the present, whether for the Earth or Mars, is fraught with uncertainty, since observations to compare with model predictions may either not be available or may provide only very indirect guidance or constraints (e.g. inferred from palaeoclimate measurements or geomorphology).

An alternative approach, that has been taken up more vigorously in recent years in the light of the discovery of a large number of extra-solar planets (Read (2011); Kaspi & Showman (2015)), makes use of a hierarchy of idealised global circulation models in which the thermodynamic/radiative forcing and boundary conditions are simplified, whilst retaining the full complexity of resolved dynamical processes. This approach allows the investigator to explore the sensitivity and dependence of the gross properties of the large-scale atmospheric circulation to/on a range of physical parameters, such as the planetary size, rotation rate, distance from the Sun and radiative opacity, provided care is taken to ensure the robustness and convergence of the numerical simulations. The simplifications made to the physical parameterizations will inevitably mean that such simplified model simulations can only represent the circulation of real planetary atmospheres with approximate quantitative accuracy (e.g. because of non-gray effects in realistic radiative transfer, the effects of moisture and latent heat, or effects due to topography). Nevertheless, such models may still represent enough of the complexity of a real atmosphere to capture the key structure of the circulation in order to make meaningful comparisons and to deduce useful trends by mapping the dependence of the style and intensity of the circulation on certain key parameters, ideally in universal dimensionless form.

In the case of Mars, it is well known that its climate and circulation exhibits many features in common with the Earth, such as a tropical Hadley circulation and a mid-latitude baroclinic storm zone in each hemisphere. But the Martian atmospheric circulation also differs from the Earth's in various ways, notably the increased dominance of thermal tides, more regular and coherent baroclinic cyclones, and increased importance of seasonal effects and the role of dust and aerosols. Although some studies have shed some light on these issues through use of models tailored to make relatively realistic simulations of the Martian or terrestrial climate, it is of interest to put both planets (and others in the Solar System and beyond) into a broader context through study of more idealised models. In this study, therefore, we present results from a series of model simulations using a simplified GCM in which a range of parameters are varied in order to identify those most important for determining the style and intensity of the circulation and to map their dependence.

Model and experiment design

The model used is the Portable University Model of the Atmosphere (PUMA; e.g. see Fraedrich et al. (1998); von Hardenberg et al. (2000)). PUMA represents the dynamical core of a spectral atmospheric general circulation model (AGCM), based on the work of Hoskins & Simmons (1975). The dry primitive equations on a sphere are integrated using the spectral transform method (Orszag (1970)). Linear terms are evaluated in the spectral domain while nonlinear products are calculated in grid point space. Temperature, divergence, vorticity, and the logarithm of the surface pressure are the prognostic variables. The vertical is divided into 10 equally spaced σ levels (where $\sigma = p/p_s$, where p and p_s denote the pressure and the surface pressure, respectively). The integration in time is carried out with a filtered leap-frog semi-implicit scheme (Robert (1966)).

Diabatic heating and cooling is represented by either by linear relaxation towards a prescribed zonally symmetric temperature distribution (designated PUMA-S) or using a two band, semi-gray radiation scheme in the standard two-stream approximation, in which short wavelength (visible and UV) and long wavelength (thermal infrared) radiation are treated separately with a single absorption coefficient, k_{sw} and k_{lw}, for each (cf. Heng (2011)), together with a surface albedo A. The distribution of incoming solar radiation may be prescribed to represent either the variation with latitude averaged over diurnal and seasonal timescales for a given obliquity angle, δ_o (designated the PUMA-G version) or with

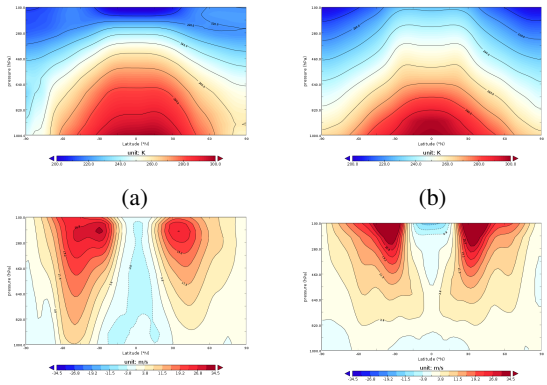

(a) (b) (c) (d)

Figure 1: Zonal and annual mean fields of temperature [(a) - (b)] and $\overline{u}$ [(c) - (d)] from an observational reanalysis (ERA-40) [(a) and (c)] and an Earth-like simulation using PUMA-G [(b) and (d)].

fully time-dependent insolation that represents diurnal and/or seasonal variations (designated PUMA-GT). The thermal inertia of the surface is represented by a prescribed relaxation timescale, τ_S, and surface dissipation is represented by a Rayleigh friction with timescale τ_f in the lowest two atmospheric layers.

Although such a simple model makes use of a radiative transfer scheme that neglects many subtle, non-gray features of real atmospheres, such as those of the Earth or Mars, the absence of such realistic details (as well as details of boundary layer structure and topography) does not prevent the model from capturing many of the key properties of the observed atmospheric circulation and structure. Figure 1, for example, compares the observed zonal mean circulation of the Earth's atmosphere ((a) and (c)) with an equilibrated PUMA-G simulation for an Earth-like planet with similar insolation, planetary size and rotation rate as the Earth. Apart from the absence of a realistic stratosphere, the SGCM represents a reasonable equator-pole thermal contrast in the tropopshere and the formation of upper level sub-tropical and mid-latitude eddy-driven zonal jets. The thermal structure of the Martian atmosphere is also captured surprisingly well by the simple 2-band semi-gray radiation scheme, as illustrated in Figure 2, provided some allowance is made for the visible opacity associated with suspended dust.

In exploring parameter space, the following nondimensional parameters are effectively varied:

- Thermal Rossby number: $\mathcal{R}o = R\Delta_H/((2\Omega a)^2$, where R is the universal gas constant, Δ_H is the average equator to pole potential temperature difference, Ω is the planetary rotation rate, and a is the planetary radius.
- Ekman number: $Ek = (2\Omega\tau_f)^{-1}$.

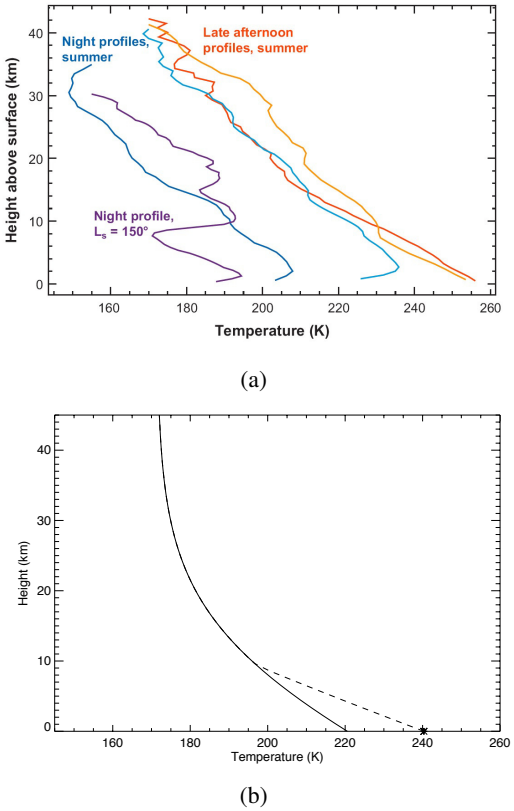

(a)

(b)

Figure 2: Comparison of observed temperature profiles in the Martian atmosphere from radio-occultation profiles ((a) from Hinson (2006)) and a radiative equilibrium profile under Martian conditions, simulated by the PUMA-G semi-gray radiation scheme (b) with a convectively adjusted profile near the ground shown with a dashed line.

- Atmospheric and surface diurnal thermal relaxation parameters: $\mathcal{A}_a = \tau_{rot}/\tau_{rad}$, and $\mathcal{A}_S = \tau_{rot}/\tau_S$, where $\tau_{rot} = 2\pi/\Omega$ and the atmospheric radiative equilibrium timescale, τ_{rad} can be approximated by $\tau_{rad} \simeq p_s c_p/(4(2-\epsilon)\sigma_B \overline{T}^3 g)$, which can be most effectively varied by either varying the surface pressure, p_s or mean absolute temperature, $\overline{T}$.
- Seasonality parameters: $\alpha_a = \tau_y/\tau_{rad}$ and $\alpha_S = \tau_y/\tau_S$, where τ_y is the orbital period.
- Longwave optical depth to space from the surface, $\tau_{lw} = \int_0^{p_s} k_{lw} dp/g$, and the corresponding shortwave opacity τ_{sw}.
- Greenhouse Parameter:

$$\mathcal{G} = (\tau_{lw} - \tau_{sw})/(\tau_{lw} + \tau_{sw}),$$

which varies between ± 1 with $\mathcal{G} = +1$ corresponding to a "perfect" greenhouse (transparent

at short wavelengths and optically thick(er) in the infrared) and $\mathcal{G} = -1$ corresponding to an anti-greenhouse atmosphere which is optically thick(er) in the visible and transparent in the infrared.

- Surface albedo: η_S.
- Planetary obliquity: ϵ_o

Circulation regimes

The use of such a simplified set of GCMs allows the model climate state to be defined by a small enough set of dimensionless control parameters to allow the exploration of its parameter space and the mapping of the conditions under which different equilibrated atmospheric circulation regimes occur. For many purposes, the most important dimensionless parameters determining the style of circulation are the Thermal Rossby number, Ekman number and thermal relaxation parameters (for a given planetary obliquity). Figure 3 shows a typical regime diagram mapping the main circulation regimes as a function of $\mathcal{R}o$ and Ek^{-1} for an Earth-like planet with obliquity $\epsilon_o = 23^\circ$ and radiative parameters appropriate for the Earth or Mars but without diurnal or seasonal cycles.

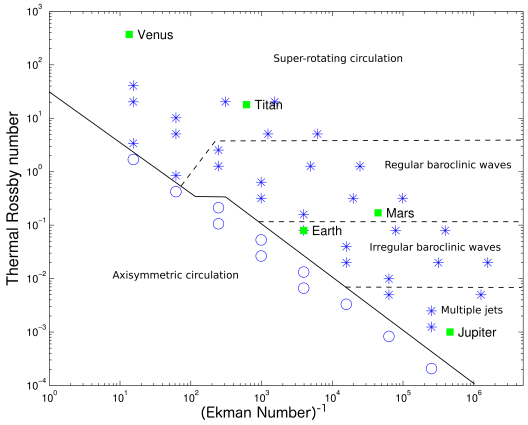

Figure 3: Regime diagram showing the various circulation regimes with respect to characteristic dimensionless parameters ($\mathcal{R}o$ and Ek^{-1}) from a set of simulations using the PUMA-S model. Individual simulations are located by stars and circles, with circles representing axisymmetric flow. The approximate location in parameter space of some Solar System planets (Earth, Mars, Titan, Jupiter, Uranus and Neptune) are labeled. The solid line delineates the boundary between axisymmetric circulations and circulations with wavy/turbulent flows. The dashed lines indicate the boundaries between different circulation regimes within the wavy/turbulent region.

This shows a clear sequence of transitions between regimes from a strongly super-rotating zonal flow at low planetary rotation through increasingly complex, baroclinically unstable regimes towards multiple jet flows at the highest rotation rates. Earth and Mars are seen to be located within the baroclinically unstable regimes, with Mars located just within a regular wave regime and the Earth in a more chaotic, irregular regime. The regular wave regime is well established in the absence of diurnal forcing and consists of almost monochromatic, zonally travelling waves at mid-latitudes. As illustrated in Figure 4, however, the zonal wavenumber is not unique but may also depend on parameters such as $\mathcal{R}o$ and Ek but also initial conditions, with hysteretic transitions between wavenumbers.

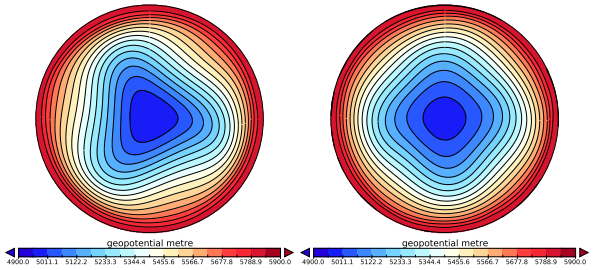

(a) (b)

Figure 4: Two examples of mid-level horizontal streamfunction fields within the regular baroclinic wave regime at $\mathcal{R}o \simeq 0.2$.

Seasonal and diurnal effects

Although the circulation of the Martian atmosphere has a number of features in common with the SGCM simulations obtained at the same values of $\mathcal{R}o$ and Ek with diurnally- and seasonally-averaged thermal forcing, there are a number of important differences, especially around the solstice seasons. This is because, unlike on Earth (over the oceans, which cover much of the surface), the thermal response timescales of both the surface and atmosphere are much shorter than the Martian year. The surface thermal inertia, in particular, plays a vital role in determining the way in which the circulation responds to the varying insolation during the year. This is well illustrated in Figure 5, which shows the zonal mean temperature field from PUMA-GT runs with a full seasonal cycle, averaged over just 5 sols. FIelds are sampled around northern winter solstice for different values of α_S, ranging from 0.16 (similar to Earth, with an ocean mixed layer at the surface) to 16 (more similar to Mars, with a rocky or sandy surface).

For diurnal effects, $\mathcal{A}_S$ and $\mathcal{A}_a$ are both relatively large so the diurnal response of both surface and atmosphere to the day-night contrast in radiative forcing is large compared to Earth, leading to a strong thermal tide throughout the atmosphere. Such large amplitude

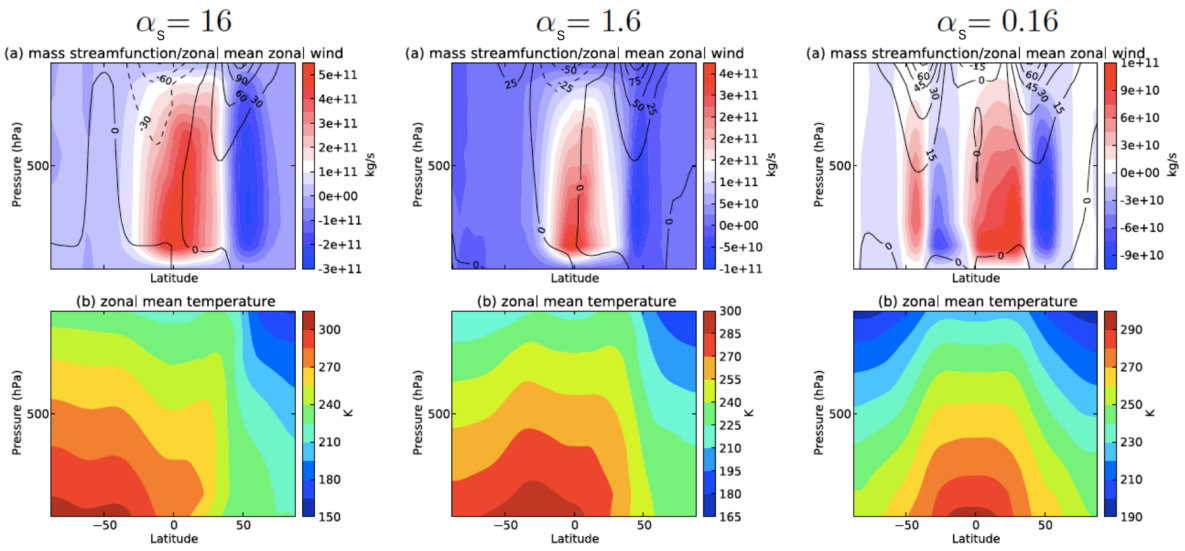

Figure 5: Comparison of seasonal and zonal mean temperature fields in simulations of a terrestrial-type planet with different values of α_S. Each frame shows a 5-sol mean, sampled at a time near northern winter solstice in equilibrated runs with a full seasonal cycle (with $\epsilon_o = 23.5°$).

tides are well known to lead not only to strong day-night thermal effects but important dynamical impacts on the synoptic-scale dynamics (Collins et al. (1996)).

These factors will be reviewed and contrasted between Mars, Earth and other planets, with particular emphasis on the dynamics of their atmospheric circulation and comparisons within the parameter space of simple GCM simulations using PUMA-G and PUMA-GT.

Acknowledgements

The authors would like to acknowledge the use of the University of Oxford Advanced Research Computing (ARC) facility in carrying out this work (`http://dx.doi.org/10.5281/zenodo.22558`), the UK Science and Technology Facilities Council, the UK Space Agency and the European Space Agency.

References

Collins, M., Lewis, S. R., Read, P. L., & Hourdin, F. (1996). Baroclinic wave transitions in the Martian atmosphere. *Icarus*, **120**, 344–357.

Fraedrich, K., Kirk, E., & Lunkeit, F. (1998). Puma: Portable University Model of the Atmosphere. *Deutsches Klimarechenzentrum Technical Report*, **16**.

Heng, K. (2011). Atmospheric circulation of tidally locked exoplanets: II. Dual-band radiative transfer and convective adjustment. *Mon. Not. R. Astron. Soc.*, **28**, 1–28.

Hinson, D. P. (2006). Radio occultation measurements of transient eddies in the northern hemisphere of Mars. *J. Geophys. Res.*, **111**, E05002.

Hoskins, B. J. & Simmons, A. J. (1975). A multi-layer spectral model and the semi-implicit method. *Quart. J. R. Meteor. Soc.*, **101**, 637–655.

Kaspi, Y. & Showman, A. P. (2015). Atmospheric dynamics of terrestrial exoplanets over a wide range of orbital and atmospheric parameters. *Astrophys. J.*, **804**, 60.

Orszag, S. A. (1970). Transform method for calculation of vector coupled sums: Application to the spectral form of the vorticity equation. *J. Atmos. Sci.*, **27**, 890–895.

Read, P. L. (2011). Dynamics and circulation regimes of terrestrial planets. *Plan. Space Sci.*, **59**, 900–914.

Robert, A. (1966). The integration of a low order spectral form of the primitive meteorological equations. *J. Meteorol. Soc. Jpn.*, **44**, 237–245.

von Hardenberg, J., Fraedrich, K., Lunkeit, F., & Provenzale, A. (2000). Transient chaotic mixing during a baroclinic life cycle. *Chaos*, **10**, 122–134.